Jacob Graham

# Design and Construction of a Time-of-Flight Mass Spectrometer and Studies of Resonance Enhanced Multiphoton Ionization of Methyl Iodide

Outline


Abstract

I. Time-of-Flight Mass Spectroscopy
   a. Fundamentals
   b. Vacuum Considerations

II. Design of a Time-of-Flight Mass Spectrometer
   a. Overview
   b. Source Region
   c. Nd:YAG & Dye Laser
   d. Timing
   e. Pulse Valve & Pickup Cell
   f. Detector
   g. LabView

III. Mass Spectrum of $CH_3I$

IV. Multiphoton Ionization
   a. Resonant versus Non-Resonant
   b. States of $CH_3I$
   c. REMPI Spectra

V. Conclusions

VI. Acknowledgements

VII. References

Abstract

Gas phase spectroscopy is an advantageous form of spectroscopy in that it allows cooled, free species to be studied without solvent effects. The selective power of a mass spectrometer is useful with gas phase spectroscopy as it can create and isolate molecular systems for study that would be impossible to study in bulk phase. Here, a Wiley-McLaren type time-of-flight mass spectrometer is designed and constructed. Focusing conditions and design considerations are discussed. Mass spectra of $CH_3I$ are presented along with a Resonance Enhanced Multiphoton Ionization (REMPI) study involving transitions through the E excited electronic state.

## I. Time-of-Flight Mass Spectroscopy

### a. Fundamentals

In time-of-flight mass spectroscopy (TOFMS), ions are accelerated with equal amounts of kinetic energy via an electric field which results in different masses of identical charge having varying velocities. TOFMS exploits this relationship between mass and velocity. The kinetic energy of a charged particle in an electric field can be described by the following equation, where charge q in a field of voltage E is accelerated a distance s.

$$KE = qEs = \tfrac{1}{2}mv^2$$

Due to the inverse relationship between mass and velocity, ions accelerated in a uniform, fixed electric field will separate into packets. Each packet has a uniform mass to charge ratio, a unique velocity and, if detected at a finite distance, arrival time.[1] This interpretation neglects several important aspects of a typical gaseous ion source. One aspect is that a gaseous source region will produce ions with a range of starting positions. This implies a distribution of kinetic energy values for ions of the same mass to charge ratio which reduce overall resolution as the spread of arrival times for each mass packet increases.

In 1955, a paper by Wiley and McLaren introduced many modern aspects of TOFMS such as spatial focusing.[2] This Wiley-McLaren focusing involves two sequential acceleration regions. This configuration, shown in Figure 1, confers several advantages. The spatial focal point of ions with the same m/z value can be tuned to an instruments particular drift distance D by manipulating the accelerating voltages. This focusing also allows a distribution of starting positions to focus at the detector resulting in a higher resolution instrument.[3]

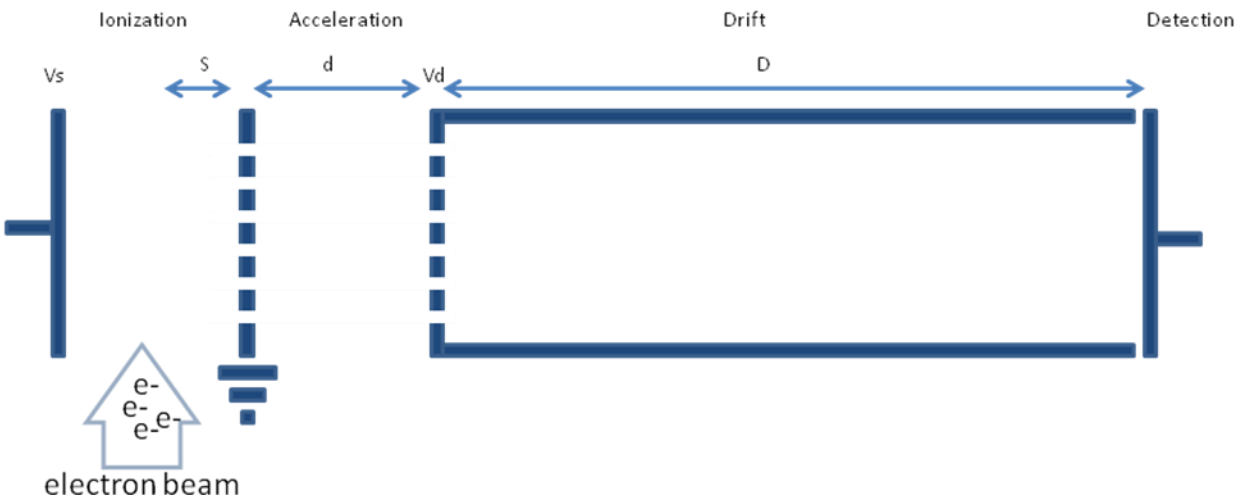


Figure 1 – Design of a Wiley-McLaren type TOFMS[2]

**b. Vacuum Considerations**

Since particles loose energy through collisions with gas molecules, a certain vacuum requirement is imposed on any region of a mass spectrometer that an ion must travel freely through. The mean free path of a particle at a certain pressure is given by:

$$L = (k\,T) / (2^{1/2}\,\rho\,d\,\sigma)$$

Where k is the Boltzmann constant, T is the temperature in kelvins, ρ is the pressure in pascals, σ is the collision cross section with $\sigma = \pi d^2$ and d is the sum of the radii of the ion and colliding ion. Given average conditions where $k = 1.38 \times 10^{-21}$ J $K^{-1}$, T ~ 300 K, $\sigma \sim 45 \times 10^{-20}$ $m^2$, it can be shown that at a typical operating pressure of $10^{-6}$ Torr where 1 Torr = 133.3 Pa, the mean free path of a gas molecule is about 5km.[4] When the pressure is reduced such an extent where the mean free path is much larger than the dimensions of the chamber, the process of gas flow is classified as molecular flow. Molecular flow is in contrast to viscous flow where gas molecules bunch up and constantly interact with neighbors. In molecular flow gas molecules can travel inside a chamber from wall to wall and rarely encounter each other. The movement of gas molecules in molecular flow from a region of high pressure to low pressure

is caused simply by the fact that the number of molecules leaving is proportional to the number present in a given region.[5]

Vacuum pumps capable of providing high vacuum conditions are varied in capabilities and operation. Most high vacuum pumps require backing by a mechanical pump and cannot vent directly to air. A diffusion pump is a very simple and capable high vacuum pump that uses downward angled jets of oil vapor to impart downward kinetic energy on residual gas molecules. A series of successive levels of oil vapor jets traps gas molecules deeper into the pump until they are evacuated by a backing mechanical pump. The walls of the diffusion pump are cooled with water so that as the jet of oil vapor contacts the wall it condenses and refills a reservoir at the base until it is reheated. Diffusion pumps can have very high pumping speed and are very simple to operate. The oil must be kept under constant vacuum to keep it degassed. Another commonly used pump is a turbomolecular pump. These pumps rotate a turbine at very high speeds. As the blades of the turbine impact gas molecules they impart kinetic energy on the molecule and direct it out of the vacuum chamber much like a diffusion pump accomplishes with oil vapor. A series of rotors is usually employed with each at a successively higher pressure. Turbomolecular pumps must also be backed by a mechanical pump.[5]

## II. Time-of-Flight Design

### a. Overview

The overall design of the constructed mass spectrometer consists of two vacuum chambers, a source chamber and detection chamber, connected via a flight tube. A schematic of the chamber assembly is shown in Figure 2.

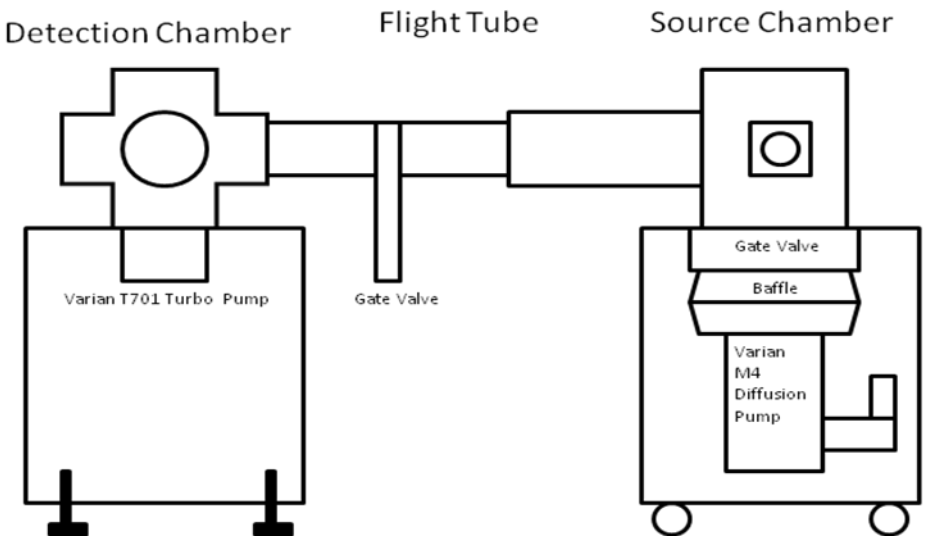


Figure 2 – Overall View

The detection chamber was assembled first using a MDC vacuum six-way cross with 8” conflat ports. The chamber was pumped with a Varian T701 Navigator Turbomolecular pump backed by a Welch 8920 Direct-Drive rotary vane mechanical pump. A detector assembly and ion gauge were attached. This chamber was connected to the source chamber via a 6” conflat flange MDC vacuum nipple and MDC gate valve. The source chamber was a custom built cylindrical vacuum chamber consisting of 8 radial o-ring sealed ports, a large o-ring sealed roof, and ASA-4 flanged port underneath. A gate valve and Varian M4 diffusion pump were connected to the bottom flange. The diffusion pump was backed by an Edwards mechanical pump. Windows, ion gauge, power feed-through and blanks with attachment points for mounting the ion optics were attached to the radial flanges. The top flange was outfitted with a o-ring sealed quick connector for use with a pulse valve. The charged particle optics, pulse valve, ion gauges and deflectors were all managed from a central electronics rack. The following sections discuss each component in detail.

**b. Source Region**

The design of the extraction/acceleration region was based largely on descriptions of Wiley & McLaren's 1955 paper[2]. The center of the chamber was designated as point of ion formation as it allowed the easiest location for present and future ionization sources, e.g. laser or electron beam. The design of the extraction region consists of a 6" x 6" aluminum plate electrically isolated from the wall of the chamber via 1 ½" ceramic standoffs. A Kapton wire from Insulator Seal connected the plate to the feedthrough. This plate was perpendicular to the ion beam line and on the side opposite of the ion formation point to the detector. This plate can also be referred to as the "pusher" plate since when charged it pushes similarly charged ions into the flight tube and towards the detector.

Across from the extraction plate and opposing the ion formation region sits another assembly referred to as the acceleration region. This consists of a grounded 6" x 6" aluminum plate with a 2 ½" hole in the center covered with a stainless steel mesh. This is attached four ceramic insulators to another 6" x 6" aluminum plate also with a 2 ½" hole in the center covered with a stainless steel mesh. This second plate is directly attached to a 6" long aluminum tube with an internal diameter of 2 ½" that is centered on the hole. This tube is surrounded by two insulating Teflon rings to permit its placement in the entrance to the flight tube and the end of the tube is covered with a stainless steel mesh. Two pairs of opposing 1 ¾" square plates that will be used as deflectors are positioned at the exit of the tube, parallel to the planned ion beam. They are attached with aluminum arms that extend from the Teflon rings. The grounded plate, acceleration plate and all four deflector plates are independently wired with Kapton wire through the feedthrough. A layout showing the position of the extraction plate, grounded plate, acceleration plate and deflectors is shown in Figure 3.

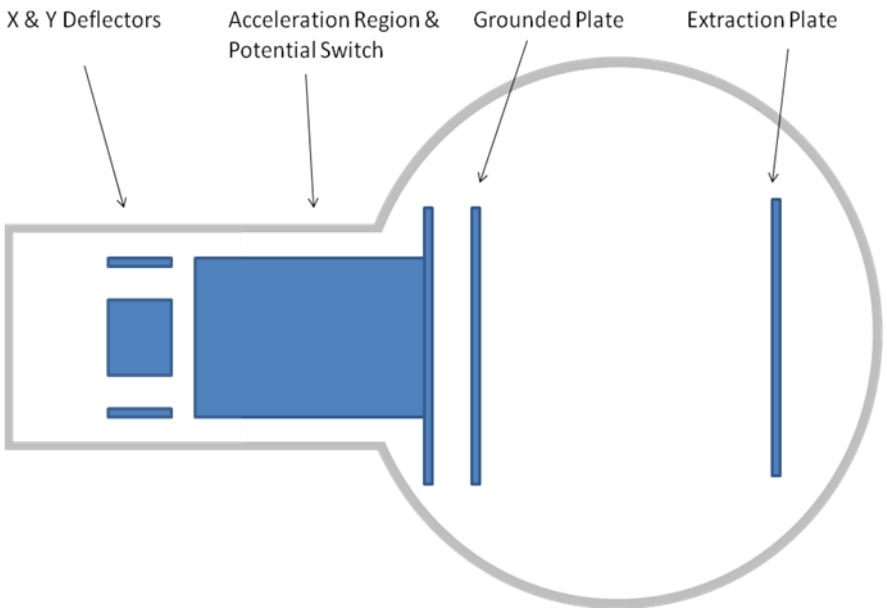


Figure 3 – Layout of Source Optics

**c. Nd:YAG and Dye Laser**

Samples that are pulsed into the source chamber are ionized through multiphoton ionization by incident radiation from a Nd:YAG pumped dye laser. A Continuum Surelite I nanosecond Nd:YAG laser is utilized as a pump source for a tunable ND 6000 dye laser. The neodymium lasing medium of a Nd:YAG laser emits 1064 nm radiation when excited from a flashlamp. Light emitted resonates in the optical cavity of the laser and reaches a maximum. A Q-Switch is operated allows the light to exit the optical cavity. The varying the delay between the flashlamp and the Q-Switch allows control of the output power of the Nd:YAG laser.

The 1064 nm radiation exiting the optical cavity of the Nd:YAG laser passes through a non-linear optical medium, a KTP crystal, which doubles the frequency through second harmonic generation. This 532 nm light is then passed through a dichroic mirror to filter out any residual 1064 nm radiation. The light is then passed into a Continuum ND 6000 dye laser. The organic dye LDS 698 is dissolved in methanol and circulated through a dye cell. The dye fluoresces from the 532 nm light and this fluorescence is collected and a narrow portion of wavelength selected with a grating. The selected

wavelength is amplified when passed through two more dye cells containing the flowing dye. Laser light emitted from the dye laser is tunable across the lasing range of the dye. This light is directed into the source chamber with several right angle BK7 glass prisms. A 20 cm focal length lens is mounted at the window of the source chamber and is used to focus the light to a small spot size.

**d. Timing**

The timing of components of a time-of-flight mass spectrometer is critical. The instrument was operated at 10 hertz. Ten times a second a packet of the sample species would be pulsed into the chamber, ionized, accelerated and detected. Timing control was achieved by a series of digital delay generators. A DG535 digital delay pulse generator by Stanford Research served as the frequency generator. Its $T_0$ output served as the start time for a timing sequence. The DG535 had two other delayed outputs that were used to control the Nd:YAG laser's flashlamp and Q-switch. The $T_0$ output was used to trigger a DEI PDG -2510 delay generator which operated the pulse valve driver. The DG535 could control the time delay between the pulse valve and the laser firing, and by controlling the time between the flashlamp and Q-switch, the laser's power. A Berkeley Nucleonics Model 8010 delay generator mounted in a NIM bin was triggered from the same pulse that operated Nd:YAG's Q-Switch. Its output pulse controlled a DEI PVX-4140 High Voltage pulse generator that powered the extraction plate. This allows a delay between ionization and extraction. A second NIM bin mounted Berkeley Nucleonics Model 8010 delay generator was triggered from the extraction pulse and was connected to a second DEI PVX-4140 High Voltage pulse generator that powered the acceleration plate. This second delay generator and high voltage pulse generator permits a variable delay between extraction and acceleration pulses. A display of each pulse over time is displayed in Figure 4 and a schematic of how each delay generator is connected is shown in Figure 5.

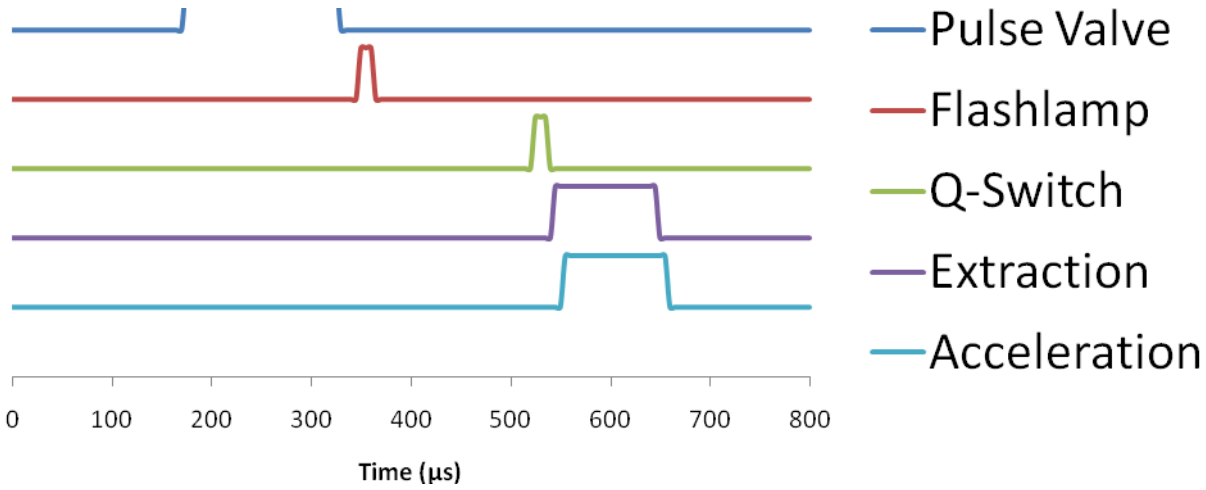


Figure 4 – Timing Diagram

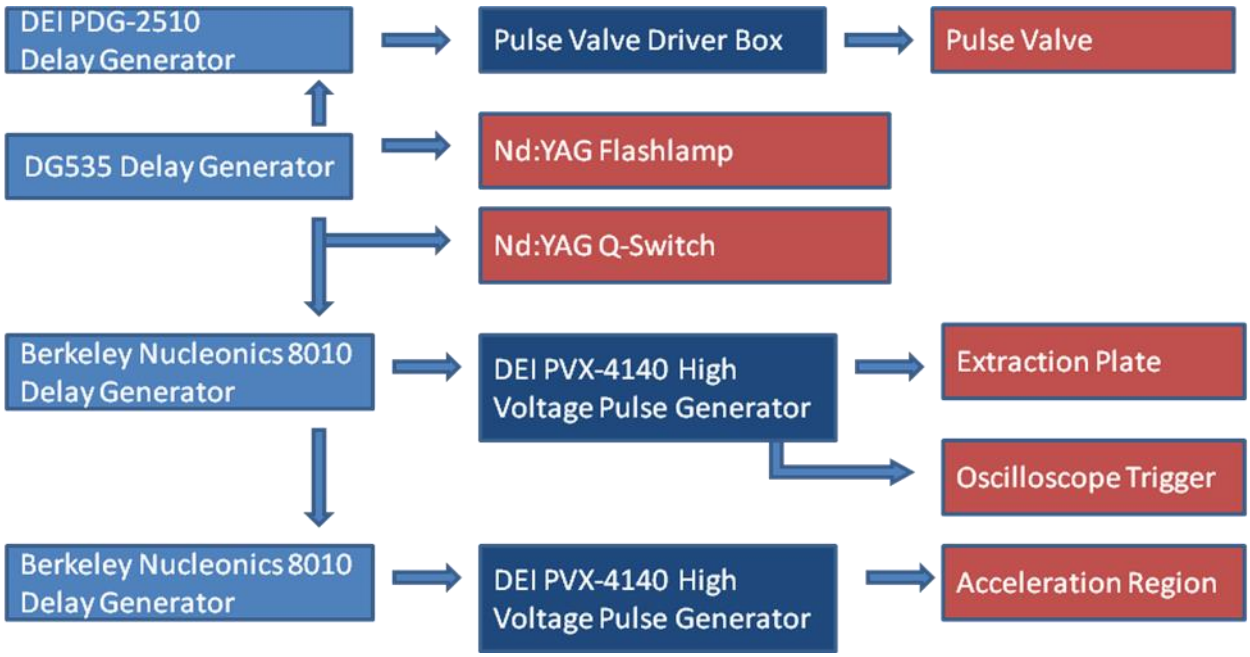


Figure 5 – Delay Generator Connections

### e. Pulse Valve & Pickup Cell

Samples are introduced to the source region through a pickup cell and pulse valve. The pickup cell consists of a borosilicate glass tube with one end sealed off and two Swagelok feedthroughs. The two feedthroughs allow a gas to be bubbled through a liquid sample and the resulting gas/sample mixture to be directed to the pulse valve. The pulse valve is a Parker Series 9 and is driven by an Iota One Driver Box. The driver box controls an electromagnet in the pulse valve which operates a Teflon poppet and permits the flow of gas for a small duration, 100-250 microseconds. Once in the chamber the gas experiences expansion and collisional cooling against the noble seed gas. Here, argon is used as the seed gas and is bubbled through a liquid sample of methyl iodide.

### f. Detector

The detector is situated in the detector chamber and marks the end of an ions flight time. A microchannel plate is an array of many small continuous dynodes that act as electron multipliers. The channels are made of a highly resistive material with a potential imposed. An ion incident on the inside wall of a microchannel causes an electron cascade through the channel which can amplify the electron count by a factor of $10^4$ to $10^7$. Ions are guaranteed to strike the wall of a microchannel as each channel is biased at an angle with respect to the surface of the plate. Microchannel plates also offer high time resolution on the order of <100 ps. This high time resolution is a critical quality of any detector for a time-of-flight mass spectrometer.[6]

Here, two Burle microchannel plates are arranged in a chevron configuration, which means that they are biased at opposite and equal degrees and placed in series. The electron cascade then falls on a conical stainless steel detector attached through a feedthrough. The signal is then passed through a fast preamp, then a fast amplifier and finally to an oscilloscope. Each microchannel plate requires 1kV bias between each side, but instead of providing this with two separate power supplies a voltage divider

circuit was utilized. A 19MΩ, 19MΩ and 2Ω resistor were arranged in series with a lead from the 2Ω grounded and 2kV applied to the first 19MΩ resistor. A potential of about 1kV exists between the 2kV and the connection between the two 19MΩ resistors and about 1kV also exists from between the two 19MΩ resistors and the connection between the 19MΩ and the 2Ω resistor. A grounded grid was installed in front of the channel plates also to protect the ions flight from fields emanating from the charged microchannel plates. A diagram of the detector is shown in Figure 6.

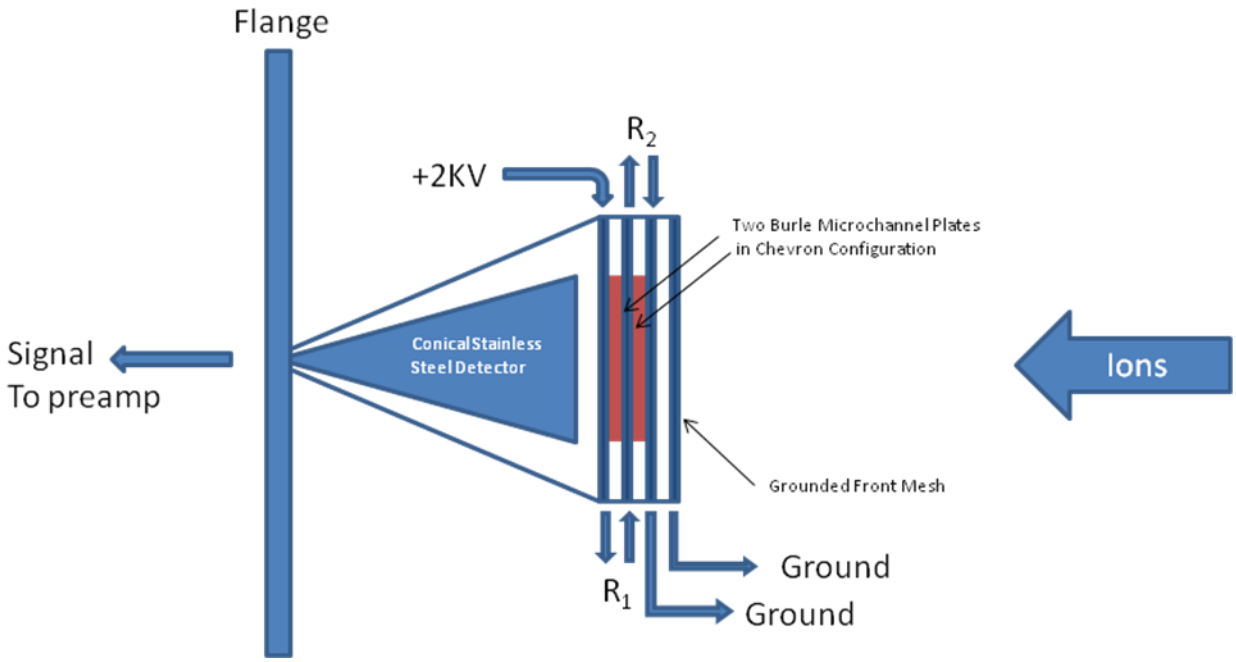


Figure 6 – Microchannel Plate Detector

**g. LabView**

After the signal is passed through a preamplifier and amplifier it is displayed on an oscilloscope. The oscilloscope is triggered by the same pulse that operates the extraction pulse so the zero time point

on the oscilloscope is the point at which the ions are first accelerated. The waveform of the oscilloscope is read over an Ethernet connection into LabView. A program was written in LabView that fulfilled the following necessary functions: read in the waveform from the oscilloscope, display a calibrated mass spectrum with a given mass & time value, integrate a certain region of the waveform to record the intensity of certain mass peak and record this data over time, communicate with the dye laser over what wavelength to scan and how many times, and plot and record the integration of a mass peak at each wavelength for several successive scans.

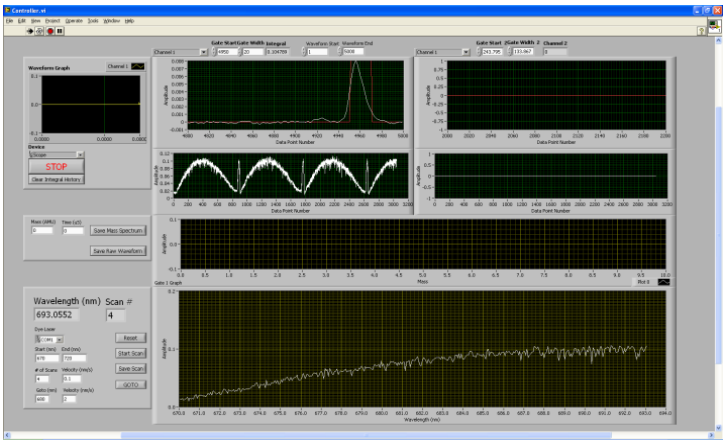


Figure 7 – LabView Screen Shot

Figure 7 shows a screenshot of the developed LabView program. The example screen shown is detecting the signal from a photodiode with respect to the wavelength of the dye laser with LDS 698 dye. An averaged power profile from four scans is show in Figure 8.

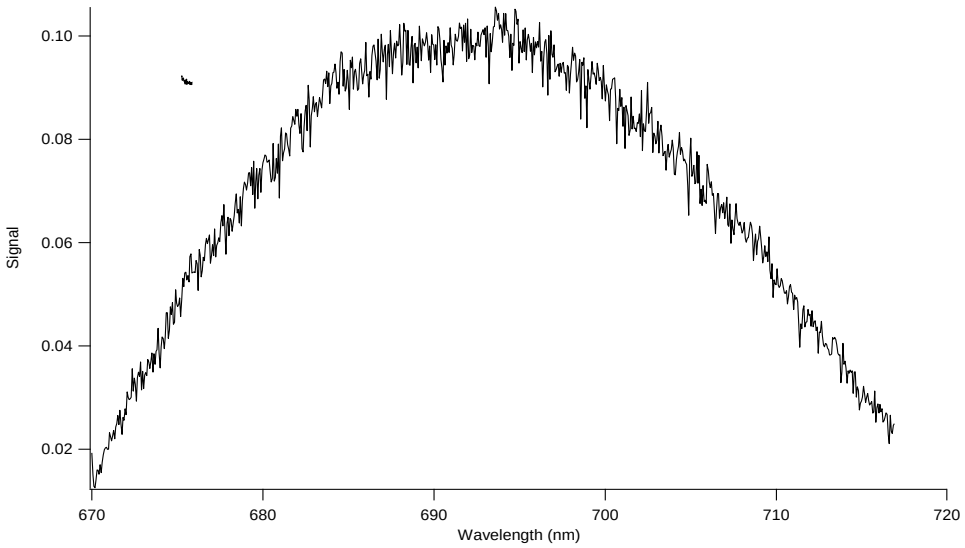


Figure 8 – Power Profile of LDS 698 Dye

### III. Mass Spectrum of $CH_3I$

The time-of-flight spectrum of $CH_3I$ seeded in Argon is presented in Figure 8. The ionization was performed by about 120 mW of 690 nm light focused by a lens with a 20cm focal length.

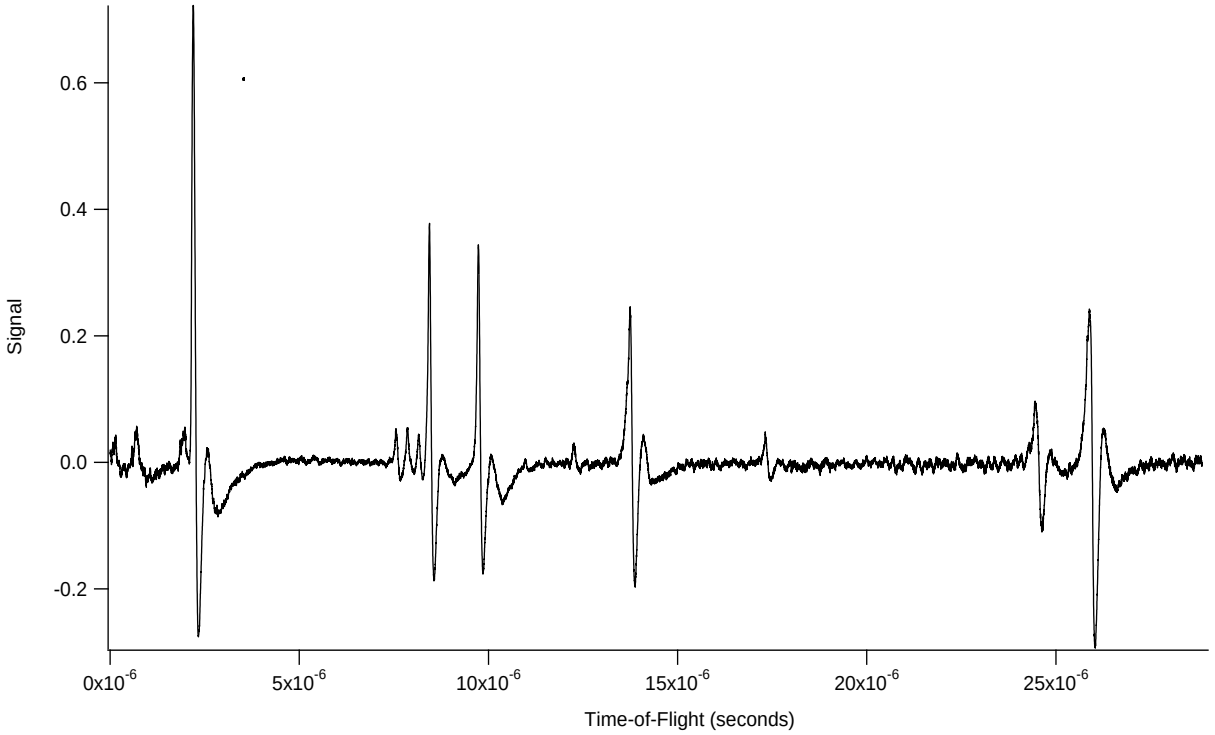


Figure 8 – Time-of-Flight spectrum of $CH_3I$

Figure 10 is magnified so peaks arising from $CH_3^+$ and associated fragments can be clearly seen.

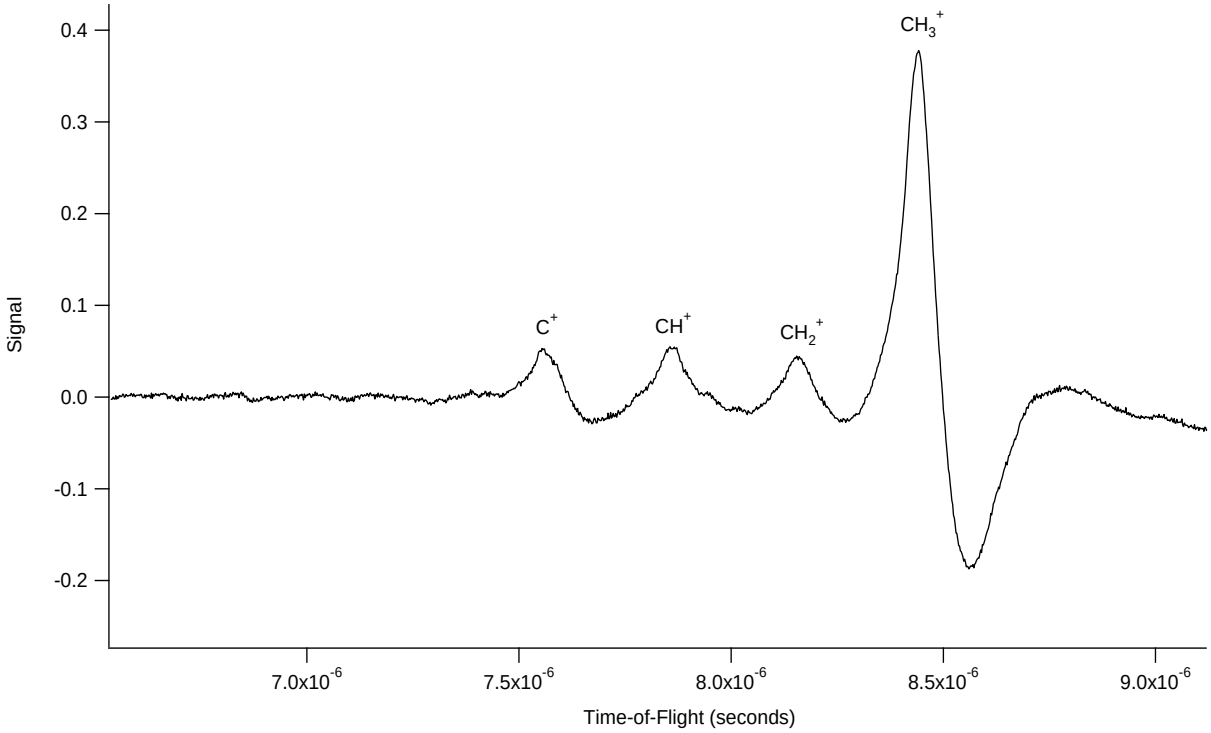


Figure 10 – Enlarged Region of Time-of-Flight Spectrum of $CH_3I$

By assigning a mass/charge ratio of 15 to the peak at 8.4 microseconds, the entire x-axis can be rescaled as function of mass. Using this new x-axis a mass spectrum of this same region is shown in Figure 11.

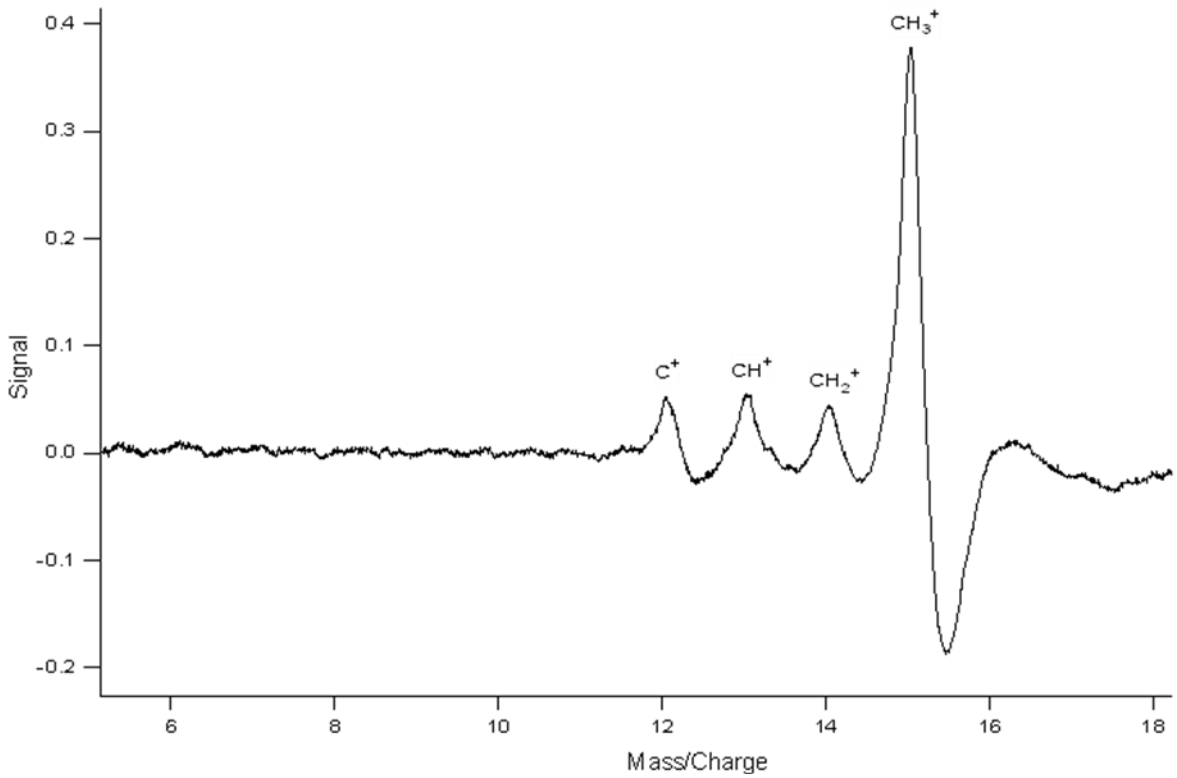


Figure 11 – Mass/Charge Spectrum of selected region of $CH_3I$

A display of the entire mass spectrum with peak assignments is presented in Figure 12.

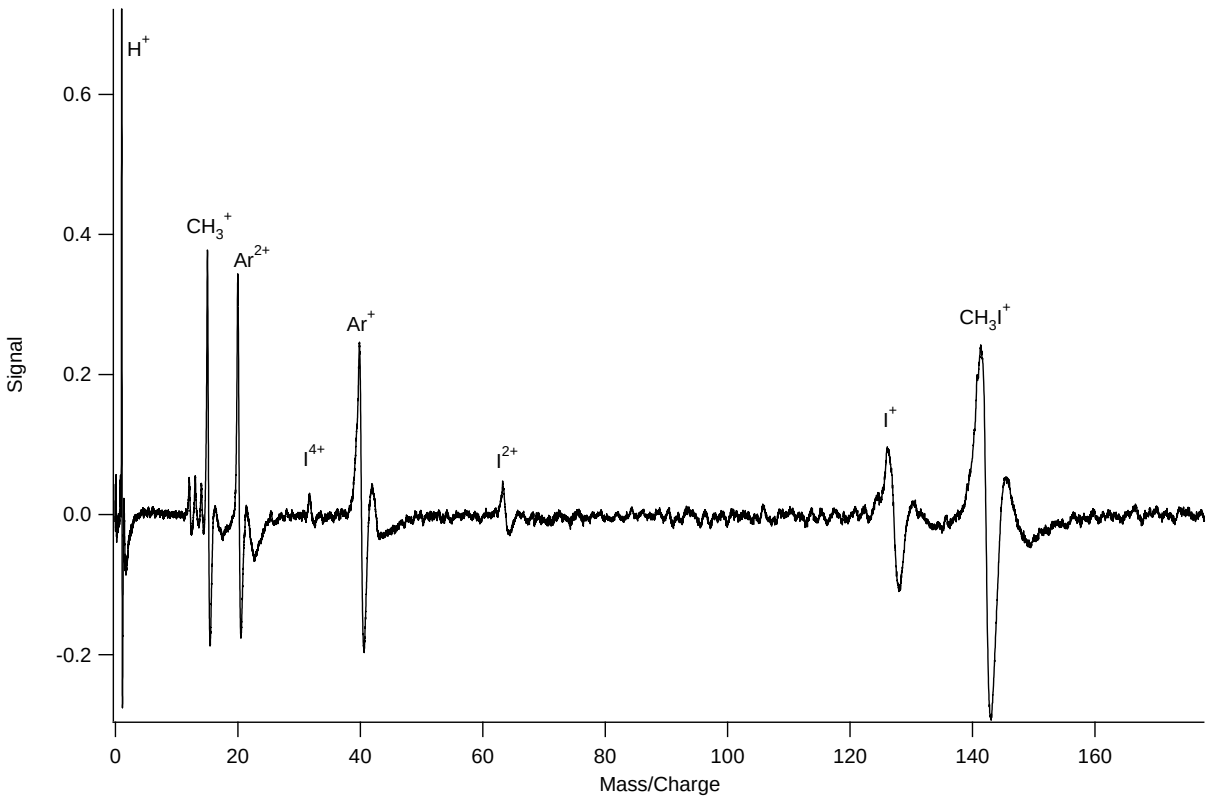


Figure 12 – Mass/Charge spectrum of $CH_3I$

From the spectrum shown in Figure 12 and its assignments it can be seen that there is a large amount of fragmentation with $H^+$, $C^+$, $CH^+$, $CH_2^+$, $CH_3^+$, $Ar^{2+}$, $I^{4+}$, $Ar^+$, $I^{2+}$, $I^+$ and the molecular ion $CH_3I^+$ all present in the spectrum.

## IV. Multiphoton Ionization

Multiphoton ionization is the ionization process used for each of the previously displayed mass spectra. In this process multiple photons strike an atom or molecule nearly simultaneously and their sum energy is enough to overcome the ionization potential. This permits photons at very high intensities from the visible region of the electromagnetic spectrum to be utilized as ionizing radiation. A feature of this ionization process is that if a certain sum of the energy of the incident photos passes through an

excited virtual state, the probability of ionizing is greater. This leads to the designation resonant and non-resonant ionization.[7] A diagram of each of these paths is shown in Figure 13.

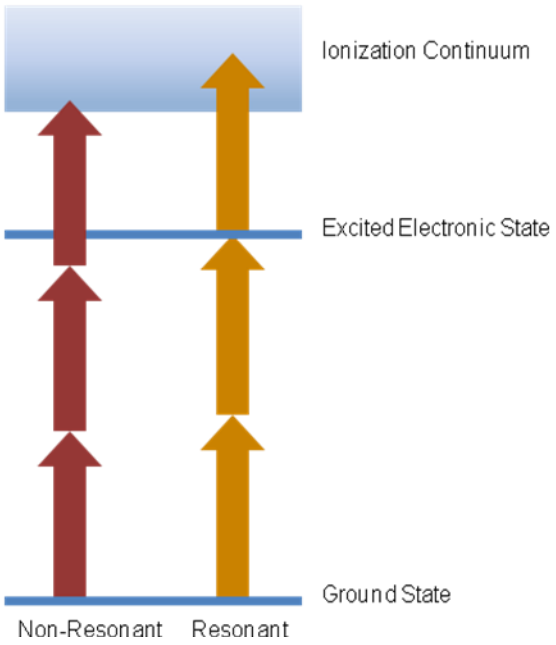


Figure 13 – Resonant and Non-Resonant Multiphoton ionization

Non-resonant ionization does not pass through an excited electronic state while resonant ionization does. By monitoring the relative signal of an ion via a mass spectrometer and scanning the wavelength of the ionization radiation an increase in intensity should correspond to an excited electronic state. From Hertzberg's *Molecular Spectra and Molecular Structure*[8] an energy level diagram for excited electronic states of methyl iodide is presented in Figure 14.

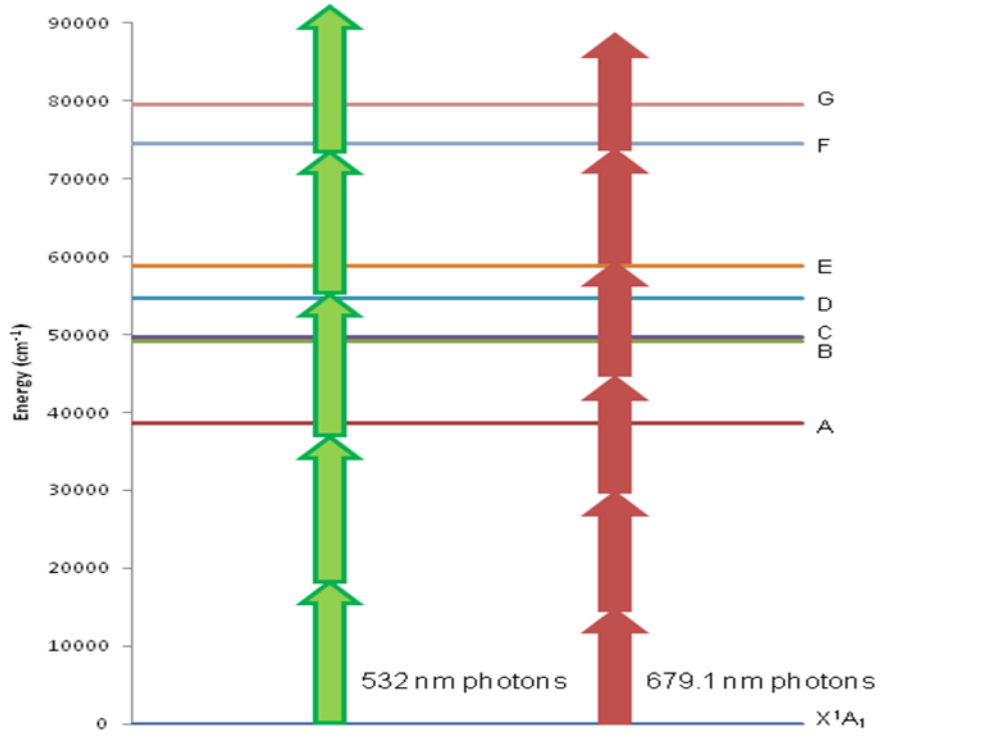


Figure 14 – Excited Electronic States of $CH_3I$

From this analysis it can be seen that a 532 nm photon does not sum exactly up to any excited electronic state. However, four photos near 679.1 nm would have the precise energy required for excitation to the E excited electronic state. An average of two scans from 690 nm to 670 nm is presented in Figure 15.

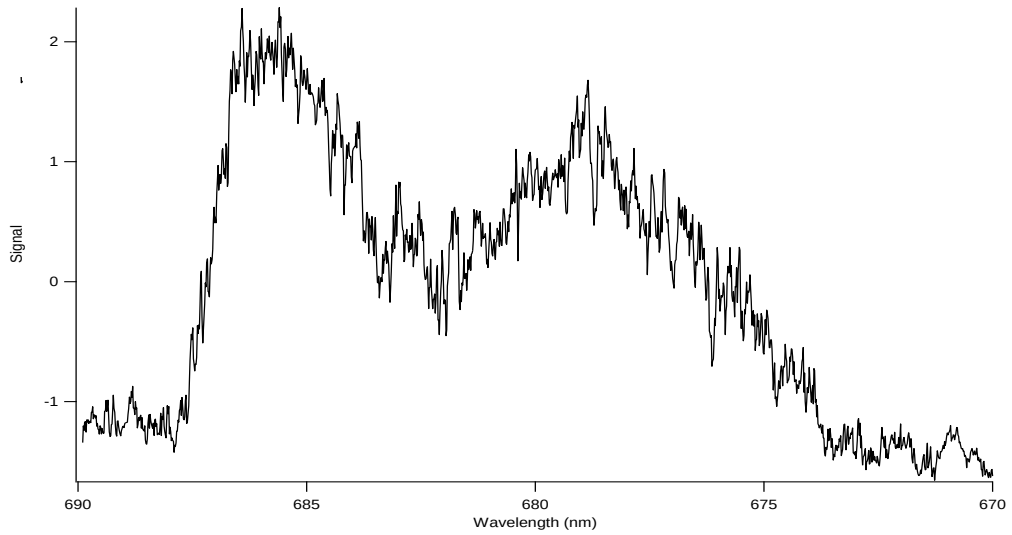


Figure 15 – REMPI spectra of $CH_3I$

The spectrum shown in Figure 15 has structure with a peak at about 685 nm and 679 nm with the peak near 679 nm corresponding to a transition through the E excited state before ionization.

## V. Conclusions

A time-of-flight mass spectrometer was designed, constructed and implemented in a resonance enhanced multiphoton ionization study of methyl iodide. Mass spectra of $CH_3I$ was recorded and analyzed with each peak assigned to a $CH_3I$ fragment. REMPI spectra of $CH_3I$ illustrated a transition through the E excited electronic state. This REMPI work was a stepping stone towards other forms of gas phase spectroscopy that require use of a time-of-flight mass spectrometer.

## VI. Acknowledgements


- Dr. Nathan Hammer
- Dr. Walter Cleland & Margo Montgomery
- Dr. Robert Compton
- Physics Machine Shop
- Hammer Group: Ashley Wright, Debra Jo Scardino, Austin Howard, Brock Sain, Ryan Gregg, Matt McDowell

## VII. References


1. M. Guilhaus, *Spectrochim. Acta Part B*, 55, 1511-525 (2000). Essential elements of time-of-flight mass spectrometry in combination with the inductively coupled plasma ion source.

2. W. C. Wiley and I. H. McLaren, *Rev. Sci. Instrum*., 26, 1150-1157 (1955). Time-Of-Flight Mass Spectrometer with Improved Resolution.

3. N. Mirsaleh-Kohan, W. D. Robertson, and R. N. Compton, *Mass Spectrom. Rev.*, 27, 237–285 (2008). Electron Ionization Time-Of-Flight Mass Spectrometry: Historical Review and Current Applications.

4. E. Hoffmann and V. Stroobant, *Mass Spectrometry Principles and Applications,* Wiley-Interscience, New York, 2007.

5. J. H. Moore, C. C. Davis, and M. A. Coplan, *Building Scientific Apparatus*, Westview Press, New York, 2002.

6. J. L. Wiza, *Nucl. Instrum. Methods Phys.*, 162, 587-601 (1979). Microchannel Plate Detectors.

7. C. Dessent and K. Mller-Dethlefs, *Chem. Rev.*, 100, 3999-4021 (2000). Hydrogen-Bonding and van der Waals Complexes Studied by ZEKE and REMPI Spectroscopy.

8. G. Herzberg, *Molecular Spectra and Molecular Structure*, Vol. 3., Prentice-Hall, New York, 1939-66.